

# Quantum Monte Carlo calculations in solids with downfolded Hamiltonians

Fengjie Ma, Wirawan Purwanto, Shiwei Zhang, and Henry Krakauer  
*Department of Physics, College of William and Mary, Williamsburg, VA 23187*

We present a systematic downfolding many-body approach for extended systems. Many-body calculations operate on a simpler Hamiltonian which retains material-specific properties. The Hamiltonian is systematically improvable and allows one to dial, in principle, between the simplest model and the original Hamiltonian. As a by-product, pseudopotential errors are essentially eliminated using a frozen-core treatment. The computational cost of the many-body calculation is dramatically reduced without sacrificing accuracy. We use the auxiliary-field quantum Monte Carlo (AFQMC) method to solve the downfolded Hamiltonian. Excellent accuracy is achieved for a range of solids, including semiconductors, ionic insulators, and metals. We further test the method by determining the spin gap in NiO, a challenging prototypical material with strong electron correlation effects. This approach greatly extends the reach of general, *ab initio* many-body calculations in materials.

PACS numbers: 71.10.-w, 02.70.Ss, 71.15.-m, 71.15.Nc

Developing accurate and efficient computational approaches for quantum matter has been a long-standing challenge. Parameter-free, material-specific many-body calculations are needed where simpler methods, such as those based on density functional theory (DFT) [1] or perturbative approaches, break down. Examples range from strongly correlated materials, such as transition metal oxides, to bond-stretching or bond-breaking in otherwise moderately correlated systems. Quantum Monte Carlo (QMC) has become increasingly important in this regard [2–10]. However, systematic and routine applications of QMC in realistic materials still face major challenges. Here we present an approach which overcomes several of the obstacles and advances the capabilities of non-perturbative ground-state calculations in correlated materials in general.

Our approach treats downfolded Hamiltonians expressed with respect to a truncated basis set of mean-field orbitals of the target system, using an auxiliary-field quantum Monte Carlo (AFQMC) method [3, 11, 12]. This allows QMC calculations to be performed with a much simpler Hamiltonian while retaining material-specific properties. The simplification, often with drastic reduction in computational cost, can extend the reach of *ab initio* computations to more complex materials. A large gain in statistical accuracy often results as well, because of the smaller range of energy scales (or many fewer degrees of freedom) which need to be sampled stochastically in the downfolded Hamiltonian.

Two other key advantages follow as a result of this approach. First, by varying the cut-off that controls the truncation of the basis orbitals, one could in principle dial between the original full-basis Hamiltonian and the simplest model. QMC calculations can be performed at each stage. This allows a systematically improvable set of calculations that connect simple models to full materials specificity. Second, the approach introduces a new way for treating core electrons, which has been a critical issue in QMC. Significant errors are often present with

the use of pseudopotential (PSP) in QMC [13, 14], due to i) inherent limitations in the accuracy of such PSPs (single-projector, generated in an atomic environment, from independent-electron calculations) [15–17], and ii) approximations in how the PSP has to be implemented in standard diffusion Monte Carlo (DMC) calculations [2, 18]. In a recent DMC study of high-pressure BN [19], the reliable determination of the equation of state (EOS) required all-electron calculations, which in most materials would not be practical. In our approach a frozen-core (FC) treatment [20] is used to essentially eliminate PSP errors.

The most fundamental issue in computations of electron correlation effects is accuracy. For QMC calculations, the fermion sign problem must, in all but a few special cases, be controlled with an approximation. The AFQMC framework, by carrying out the random walks in non-orthogonal Slater determinant space, has shown to lead to an approximation which is more accurate and less dependent on the trial wave function [3, 4, 10, 12, 17, 21, 22]. In both lattice models [23] and molecular systems [5], recent advances with AFQMC have allowed systematic accuracy in treating strongly correlated systems. The method proposed here provides an approach to seamlessly integrate these advances in the study of solids. We illustrate the approach by obtaining accurate equilibrium properties in a range of solids, including semiconductors, ionic insulators, and metals. We then show that the present approach can describe BN, with an accurate EOS extending to high pressures, without resorting to all-electron calculations. Finally, the spin gap in strongly correlated NiO is accurately determined and compared with experiment.

The construction of the downfolded Hamiltonian begins with a standard DFT calculation for the target system. This is done using a planewave basis with PSPs. (Extremely hard PSPs, e.g., He-core for third row elements or “zero-electron-core” for the first-row, are employed, if necessary, to eliminate transferability errors of

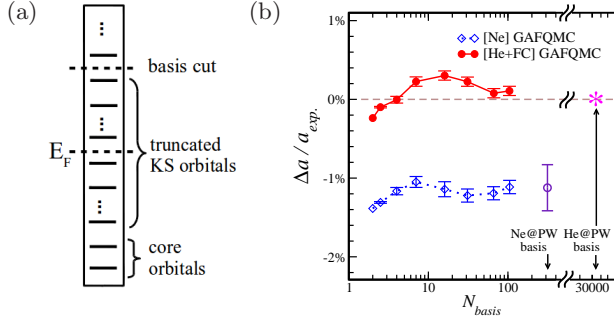


FIG. 1: (Color online) a) Illustration for basis downfolding. Solid black lines represent DFT KS orbitals. A compact basis is constructed with DFT-KS orbitals, by neglecting the less physically relevant high-energy states above a truncation energy. Deep core electrons can be frozen at the mean-field level by a frozen-core treatment. b) Error in the calculated lattice constant in Si vs. basis size. Results with standard Ne-core and a highly accurate He-core PSP plus FC are both shown. For the Ne-core PSP, the full planewave AFQMC result is indicated by the indigo open circle. For the He-core PSP, the number of planewaves required in the full calculation is indicated (note logarithmic scale).

conventional norm-conserving PSPs [20], at essentially no additional computational cost in the ensuing many-body calculations.) Planewaves are desirable at this stage, because they provide an unbiased representation of the many-body Hamiltonian. We then use the Kohn-Sham (KS) orbitals as basis set, tuned to eliminate less physically relevant high-energy virtual states and low-energy core states, as illustrated in Fig. 1a. Expressed in this basis, the effective downfolded Hamiltonian is given by one-body and two-body terms whose matrix elements are

$$K_{ij} = \langle \chi_i | \hat{K} | \chi_j \rangle; \quad V_{ijkl} = \langle \chi_i \chi_j | \hat{V} | \chi_k \chi_l \rangle \quad (1)$$

where  $|\chi_i\rangle$  is a KS orbital, the labels  $i, j, k$ , and  $l$  all run in the truncated basis set,  $\hat{K}$  includes all one-body (and constant) terms in the Hamiltonian and  $\hat{V}$  is the two-body interaction term. The matrix elements, which encode the periodicity and the Coulomb interaction in the underlying supercell [17], can be conveniently computed using fast Fourier transforms, as the orbitals  $\chi$  are given in planewaves. We use twist boundary conditions [24] on the supercell. For inversion-symmetric systems, all the matrix elements are *real* under any twist  $\mathbf{k}$ . The core states can be frozen in the corresponding KS orbitals of the solid; two-body core-valence interactions appear as one-body ion-valence terms  $K_{ij}$  and core-only interactions (one-body and two-body) contribute a constant [20].

The downfolded Hamiltonian defined in Eq. (1) is then treated using phaseless AFQMC [11] but in the molecular formalism [12, 25], which can handle any one-particle basis functions. The approach is illustrated for fcc Si in Fig. 1(b), which shows the convergence of the calculated

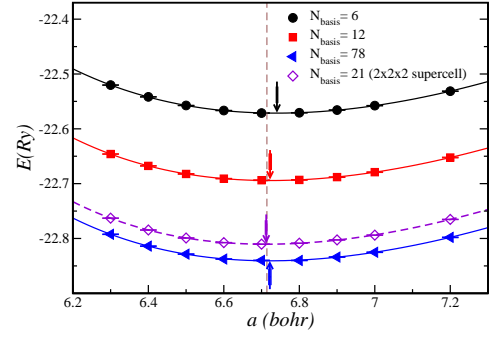


FIG. 2: (Color online) EOS of fcc diamond with different basis cut-offs,  $N_{\text{basis}}$  (per atom). The experimental lattice parameter is indicated by the vertical dashed line. The calculated equilibrium lattice constant for each curve is indicated by a solid arrow, with the width of the line showing the statistical error bar. The total energy changes with  $N_{\text{basis}}$ , but the equilibrium properties converge rapidly. Residual finite size effects are corrected and checked by calculations in the larger supercell.

equilibrium lattice constant. Results are shown for both Ne- and He-core PSPs [26]. With the Ne-core PSP, each Si atom contributes four electrons, and there are no “core electrons” in the diagram in Fig. 1a. The basis cut controls the number of KS orbitals in the truncated basis,  $N_{\text{basis}}$ . When all states are retained in the truncation, the KS orbital basis is just a unitary transformation of the original planewave basis. As  $N_{\text{basis}}$  is increased, the result converges to the full planewave AFQMC result. The statistical error bar with the downfolded Hamiltonian is much smaller, however, because many fewer auxiliary-fields need to be sampled [17, 25]. With the He-core PSP, very small radial cut-offs (0.54, 0.68, and 0.54 bohr for  $s$ ,  $p$ , and  $d$  channels, respectively) were used, which resulted in a large planewave cut-off  $E_{\text{cut}} = 600$  Ry. The  $2s$  and  $2p$  electrons are then treated as “core electrons,” frozen in their KS orbitals. As seen in Fig. 1(b), this approach (He-core plus FC) eliminates the 1.2% error in the calculated lattice constant from the Ne-core PSP. Furthermore, the calculation reaches convergence with  $\sim 100$  basis functions, more than two orders of magnitude smaller than would be required in the full planewave calculation.

The basis choice and truncation method are not unique. Possible truncation choices include a fixed number of basis functions, a fixed cut-off energy, a fixed ratio to the full basis, etc. We find that the first choice leads to the most rapid convergence in our EOS calculations. There is also considerable freedom in the choice of underlying basis. In spin-polarized systems, we generate a spin-consistent basis set by diagonalizing the  $2N_{\text{basis}} \times 2N_{\text{basis}}$  overlap matrix formed by  $\langle \chi_i^\sigma | \chi_j^{\sigma'} \rangle$ , where  $\sigma$  and  $\sigma'$  are spin indices. The resulting eigenfunctions corresponding to the largest  $N_{\text{basis}}$  eigenvalues

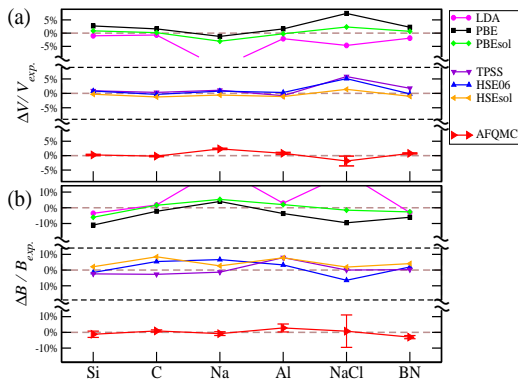


FIG. 3: Summary of calculated equilibrium volumes (a) and bulk moduli (b), shown as relative errors from experiment. Selected DFT results are also shown for reference. Zero-point effects have been subtracted from the experiments [33, 34].

are used as new “KS orbitals,” which leads to an unbiased basis set and much faster convergence, as illustrated for NiO below. Similarly, localization strategies could be applied to generate more efficient basis sets [27–29].

EOS calculations are shown in Fig. 2 for fcc diamond. The total energy decreases with increasing  $N_{\text{basis}}$ , as expected, but the overall shape of the EOS is similar. With each, a fit to the Murnaghan equation [30] is done to obtain the equilibrium lattice constant and bulk modulus. With only  $N_{\text{basis}} = 12$  per atom, the equilibrium lattice constant is essentially converged. The calculations used  $\mathbf{k} = (0.5, 0.5, 0.5)$ ; one-body and two-body finite-size corrections derived from the corresponding simulation cells [31, 32] are applied to the many-body results. As illustrated in the figure, calculations for a larger supercell were carried out to check that residual finite-size effects are smaller than the statistical errors in the final result.

As additional tests in “conventional” systems, we apply the AFQMC downfolding approach to two metals Na and Al, an ionic crystal NaCl, and BN, whose high-pressure EOS is further studied below for pressure calibration. Figure 3 summarizes all the results of calculated equilibrium properties and compares them with experiment. The calculations for NaCl and BN were analogous to those for Si and C. The calculations in bcc Na and fcc Al used twist averaging over 90 random  $\mathbf{k}$ -points [24]. He-core PSPs were used for Na and Al, together with the FC treatment as described for Si. This makes a major difference in both NaCl and Na. With a Ne-core PSP, the equilibrium volume is underestimated by  $\sim 30\%$  in Na, for example. The error is eliminated by the FC approach, which allows the semi-core  $2s$  and  $2p$  electrons to fully relax in the *target environment of the solid* at the DFT-level, before freezing them in the corresponding KS orbitals in the many-body calculation.

The agreement between downfolding AFQMC and ex-

periments [33, 35–37] is excellent. For reference, some representative DFT results are shown in Fig. 3: the top panels in (a) and (b) include results from the widely used local-density (LDA) and generalized gradient (GGA, with two flavors, PBE and a variant which is specially designed for solids and surfaces, PBEsol) approximations [38–40]; the middle panels sample more recent developments in DFT, with a meta-GGA (TPSS) and two flavors of hybrid functionals (HSE06 and HSEsol) [33, 35–37], which are highly accurate in many conventional systems but often involve empirical parameters. The AFQMC results (bottom panels) demonstrate that the new approach provides an *ab initio*, parameter-free, many-body framework that is consistently accurate. The calculations used single-determinant trial wave functions taken directly from LDA or GGA to control the sign or phase problem of the random walks in Slater determinant space [3, 11]. The systematic error from this approximation, based on extensive prior benchmarks [10, 11, 17, 22], is expected to be essentially negligible in these systems, in accord with the results in the figure. The largest uncertainty arises in NaCl and is statistical in nature. Different from the other systems, the ionic character results in valence states localized on the Cl atom. The high-energy virtual KS orbitals, which are used to capture the effect of electron interactions, are free-electron like, however. As a result, convergence of the EOS is slow and an extrapolation with respect to  $1/N_{\text{basis}}$  was needed to reach the complete basis set limit, resulting in larger uncertainty. Clearly, this can be improved by using Wannier or other localized orbitals in the downfolding.

In a more demanding test, we apply downfolding AFQMC to obtain the EOS of cubic BN for pressures up to 900 GPa ( $V \sim 0.5 V_{eq}$ ). This system has been identified as a promising material for an ultra-high pressure calibration scale [19, 44]. A recent DMC study stressed the need for all-electron (AE) calculations in order to obtain reliable results at high pressures [19]. The difficulty underscores the PSP transferability problem discussed above in the context of Na and Si, and is exacerbated by the need to apply a locality approximation in DMC to treat non-local PSPs [2, 18]. The AE treatment would be difficult to realize for heavier atoms. Our calculations freeze the  $1s$  electrons in their KS orbitals in the supercell at each volume, using extremely hard “zero-electron-core” PSPs for B and N in the downfolding procedure [45]. In most cases  $\sim 55$  states/atom were used, but larger  $N_{\text{basis}}$  calculations were done at selected volumes to extrapolate the EOS to the complete basis set limit. We applied finite-temperature corrections following Ref. 19. The calculations were done with  $\mathbf{k} = (0.5, 0.5, 0.0)$  for 8- and 16-atom supercells, with one- and two-body finite-size corrections as discussed earlier; we have confirmed that residual errors are negligible compared to the final estimated error band, especially in the high-pressure regime. As seen in Fig. 4, the cal-

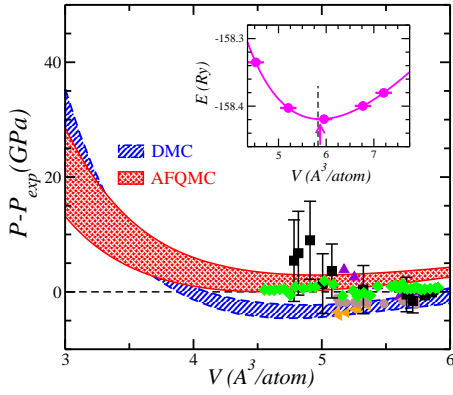


FIG. 4: (Color online) Pressure calibration and EOS in cubic BN. The main graph displays the calculated pressure vs. volume at room-temperature, using the fitted experimental curve of Ref. 34 (green diamond symbols) as a pressure reference. Different symbols are from different experiments [34, 41–43]. The shading gives the overall statistical uncertainties in the calculations. The all-electron DMC results are from Ref. 19. The inset shows the  $T = 0$  K EOS near equilibrium from AFQMC. The calculated equilibrium position is shown by the arrow. The vertical line indicates the experimental value [34, 41].

culated EOS at low pressures is in excellent agreement with experiments [34, 41–43]. The calculated equilibrium lattice constant, 6.820(3) bohr, is consistent with experimental measurements of 6.802 bohr (zero-point energy removed), as shown in the inset. The EOS at low pressures shows small but discernible discrepancies with DMC results. Possible origins include differences in the finite-temperature corrections [46], or DMC fixed-node errors, and will require further investigation. At high pressures, the two QMC results are in good agreement, providing a consistent *ab initio* pressure calibration.

As a final application, we determine the spin gap between the ferromagnetic (FM) state and the antiferromagnetic (AFM-II) ground state in NiO. Understanding and predicting magnetic properties of transition-metal oxides epitomizes the challenge of computations in quantum matter. NiO is a prototypical system for strong electron correlations. Many-body calculations of the spin gap have been limited, and DFT-based methods have yielded widely varying values [49]. We use Ne-core and He-core PSPs for Ni and O, respectively. The downfolded Hamiltonian treats the Ni 3s, 3p, 3d, 4s and O 2s, 2p electrons. A rhombohedral supercell with a lattice constant of 4.17 Å containing two formula units is used. To reduce one-body finite-size effects, we used twist-averaging with a  $4 \times 4 \times 4$  Monkhorst-Pack grid [50]. (A recent study [51] by full configuration-interaction QMC and coupled-cluster methods, with calculations at  $\mathbf{k} = \Gamma$ , obtained a gap value  $\sim 0.96$  eV.) One- and two-body finite-size corrections [32] are then applied to the many-body re-

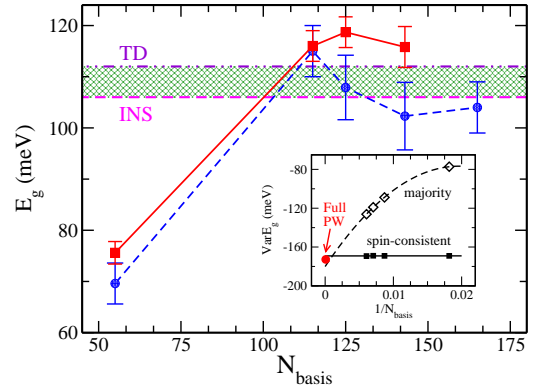


FIG. 5: Spin gap in NiO, and comparison with experiment. A smaller set of calculations (blue circles), averaging over two  $\mathbf{k}$ -points, confirms convergence with respect to basis set cutoff  $N_{\text{basis}}$ . Calculations averaging over a  $4 \times 4 \times 4$  Monkhorst-Pack grid (red squares) are used to obtain the final results. The shaded bar represents the experimental range: inelastic neutron scattering (INS) [47] (bottom line) and thermodynamic (TD) measurements [48] (top line). The inset illustrates the much faster convergence enabled by the spin-consistent basis set (see text) than using the KS orbitals from the majority spin.

sults (two-body finite-size effects are greatly reduced by cancellation, because the two phases share the same supercell). In the downfolding we use the spin-consistent basis sets discussed earlier. In the inset in Fig. 5, the variational gap value from the single-determinant trial wave functions is shown vs. the number of basis functions, for both the spin-consistent basis set and one which uses truncated KS orbitals of the majority spin. Both converge to the same infinite basis-set limit, as expected, but the former greatly accelerates convergence. Note that the variational gap (which has been averaged over  $\mathbf{k}$ -points) is actually negative, i.e., the trial wave functions identify the incorrect phase for the ground state. The AFQMC calculations correctly recover from these, and yield a final estimate of the gap of 116(3) meV, in good agreement with experiments [47, 48].

In summary, we have presented a systematic downfolding Hamiltonian approach for solids. As a first test, parameter-free calculations of equilibrium properties are demonstrated in semiconductors, metals, and ionic insulators. QMC PSP errors are eliminated without (prohibitive) all-electron calculations, as demonstrated in BN. The spin gap in strongly correlated NiO is accurately determined. The approach drastically reduces complexity and computational cost, and greatly extends the reach of *ab initio*, non-perturbative, many-body computations in complex materials. Furthermore, the framework provides a tunable connection between the full materials-specific Hamiltonian and simplified models. The downfolding approach can be generalized to carry out excited state and many-body band structure calculations, which



was recently formulated [10] in planewave AFQMC. A large number of applications are possible within the present form. Further improvements, for example by using localized virtual states or optimizing the orbitals with respect to the environments, will lead to even more general and powerful approaches.

This work is supported by DOE (DE-SC0008627 and DE-SC0001303), NSF (DMR-1409510), and ONR (N000141211042). An award of computer time was provided by the Innovative and Novel Computational Impact on Theory and Experiment (INCITE) program, using resources of the Oak Ridge Leadership Computing Facility at the Oak Ridge National Laboratory, which is supported by the Office of Science of the U.S. Department of Energy under Contract No. DE-AC05-00OR22725. We also acknowledge computing support from the computational facilities at the College of William and Mary.

- 
- [1] W. Kohn, Rev. Mod. Phys. **71**, 1253 (1999).
  - [2] W. M. C. Foulkes, L. Mitas, R. J. Needs, and G. Rajagopal, Rev. Mod. Phys. **73**, 33 (2001).
  - [3] S. Zhang, *Auxiliary-Field Quantum Monte Carlo for Correlated Electron Systems*, Vol. 3 of *Emergent Phenomena in Correlated Matter: Modeling and Simulation*, Ed. E. Pavarini, E. Koch, and U. Schollwöck (Verlag des Forschungszentrum Jülich, 2013).
  - [4] W. A. Al-Saidi, S. Zhang, and H. Krakauer, J. Chem. Phys. **127**, 144101 (2007).
  - [5] W. Purwanto, H. Krakauer, and S. Zhang, arXiv:1410.3505.
  - [6] L. Shulenburger and T. R. Mattsson, Phys. Rev. B **88**, 245117 (2013).
  - [7] J. c. v. Kolorenč and L. Mitas, Rep. Prog. Phys. **74**, 026502 (2011).
  - [8] L. K. Wagner, J. Phys.: Condens. Matter **19**, 343201 (2007).
  - [9] L. K. Wagner and P. Abbamonte, Phys. Rev. B **90**, 125129 (2014).
  - [10] F. Ma, S. Zhang, and H. Krakauer, New J. Phys. **15**, 093017 (2013).
  - [11] S. Zhang and H. Krakauer, Phys. Rev. Lett. **90**, 136401 (2003).
  - [12] W. A. Al-Saidi, S. Zhang, and H. Krakauer, J. Chem. Phys. **124**, 224101 (2006).
  - [13] S. Sorella, M. Casula, L. Spanu, and A. Dal Corso, Phys. Rev. B **83**, 075119 (2011).
  - [14] R. G. Hennig, A. Wadehra, K. P. Driver, W. D. Parker, C. J. Umrigar, and J. W. Wilkins, Phys. Rev. B **82**, 014101 (2010).
  - [15] J. R. Trail and R. J. Needs, J. Chem. Phys. **122**, 174109 (2005).
  - [16] M. Burkatzki, C. Filippi, and M. Dolg, J. Chem. Phys. **126**, 234105 (2007).
  - [17] M. Suewattana, W. Purwanto, S. Zhang, H. Krakauer, and E. J. Walter, Phys. Rev. B **75**, 245123 (2007).
  - [18] L. Mit, E. L. Shirley, and D. M. Ceperley, J. Chem. Phys. **95**, 3467 (1991).
  - [19] K. P. Esler, R. E. Cohen, B. Militzer, J. Kim, R. J. Needs, and M. D. Towler, Phys. Rev. Lett. **104**, 185702 (2010).
  - [20] W. Purwanto, S. Zhang, and H. Krakauer, J. Chem. Theory Comput. **9**, 4825 (2013).
  - [21] W. A. Al-Saidi, H. Krakauer, and S. Zhang, Phys. Rev. B **73**, 075103 (2006).
  - [22] W. Purwanto, H. Krakauer, and S. Zhang, Phys. Rev. B **80**, 214116 (2009).
  - [23] C.-C. Chang and S. Zhang, Phys. Rev. Lett. **104**, 116402 (2010).
  - [24] C. Lin, F. H. Zong, and D. M. Ceperley, Phys. Rev. E **64**, 016702 (2001).
  - [25] W. Purwanto, H. Krakauer, Y. Virgus, and S. Zhang, J. Chem. Phys. **135**, 164105 (2011).
  - [26] E. J. Walter, *Opium: pseudopotential generation project*, <http://opium.sourceforge.net>.
  - [27] I.-M. Høyvik, K. Kristensen, T. Kjærgaard, and P. Jørgensen, Theor. Chem. Acc. **133**, 1417 (2013).
  - [28] A. Grüneis, G. H. Booth, M. Marsman, J. Spencer, A. Alavi, and G. Kresse, J. Chem. Theory Comput. **7**, 2780 (2011).
  - [29] N. Marzari, A. A. Mostofi, J. R. Yates, I. Souza, and D. Vanderbilt, Rev. Mod. Phys. **84**, 1419 (2012).
  - [30] F. D. Murnaghan, Proc. Natl. Acad. Sci. USA **30**, 244 (1944).
  - [31] H. Kwee, S. Zhang, and H. Krakauer, Phys. Rev. Lett. **100**, 126404 (2008).
  - [32] F. Ma, S. Zhang, and H. Krakauer, Phys. Rev. B **84**, 155130 (2011).
  - [33] L. Schimka, J. Harl, and G. Kresse, J. Chem. Phys. **134**, 024116 (2011).
  - [34] F. Datchi, A. Dewaele, Y. Le Godec, and P. Loubeyre, Phys. Rev. B **75**, 214104 (2007).
  - [35] V. N. Staroverov, G. E. Scuseria, J. Tao, and J. P. Perdew, Phys. Rev. B **69**, 075102 (2004).
  - [36] V. N. Staroverov, G. E. Scuseria, J. Tao, and J. P. Perdew, Phys. Rev. B **78**, 239907(E) (2008).
  - [37] P. Hao, Y. Fang, J. Sun, G. I. Csonka, P. H. T. Philipsen, and J. P. Perdew, Phys. Rev. B **85**, 014111 (2012).
  - [38] J. P. Perdew and A. Zunger, Phys. Rev. B **23**, 5048 (1981).
  - [39] J. P. Perdew, K. Burke, and M. Ernzerhof, Phys. Rev. Lett. **77**, 3865 (1996).
  - [40] J. P. Perdew, A. Ruzsinszky, G. I. Csonka, O. A. Vydrov, G. E. Scuseria, L. A. Constantin, X. Zhou, and K. Burke, Phys. Rev. Lett. **100**, 136406 (2008).
  - [41] A. F. Goncharov, J. C. Crowhurst, J. K. Dewhurst, S. Sharma, C. Sanloup, E. Gregoryanz, N. Guignot, and M. Mezouar, Phys. Rev. B **75**, 224114 (2007).
  - [42] V. L. Solozhenko, D. Husermann, M. Mezouar, and M. Kunz, Appl. Phys. Lett. **72**, 1691 (1998).
  - [43] E. Knittle, R. M. Wentzcovitch, R. Jeanloz, and M. L. Cohen, Nature **337**, 349 (1989).
  - [44] Y. Tian, B. Xu, D. Yu, Y. Ma, Y. Wang, Y. Jiang, W. Hu, C. Tang, Y. Gao, K. Luo, et al., Nature **493**, 385 (2013).
  - [45] The radial cut-offs are 0.58 bohr for *s* and *p* channels of B, and 0.61 bohr for those of N, resulting in planewave cut-off 600 Ry.
  - [46] Finite temperature contribution is obtained from the difference between our standard 0K DFT calculation and the room temperature DFT result in Ref. 19. PSPs are generated with OPIUM using the same type of exchange-correlation functional (WCGGA). The radial cut-offs are 1.08 bohr for *s*, *p*, and *d* channels of B, and 1.18, 1.25, and 1.25 bohr for those of N, resulting in planewave cut-off

- 85 Ry. Partial core correction is included.
- [47] M. T. Hutchings and E. J. Samuelsen, Phys. Rev. B **6**, 3447 (1972).
  - [48] R. Shanker and R. A. Singh, Phys. Rev. B **7**, 5000 (1973).
  - [49] T. Archer, C. D. Pemmaraju, S. Sanvito, C. Franchini, J. He, A. Filippetti, P. Delugas, D. Puggioni, V. Fiorentini, R. Tiwari, et al., Phys. Rev. B **84**, 115114 (2011).
  - [50] H. J. Monkhorst and J. D. Pack, Phys. Rev. B **13**, 5188 (1976).
  - [51] G. H. Booth, A. Gruneis, G. Kresse, and A. Alavi, Nature **493**, 365 (2013).